# Cyril Dejean, Christian E. Gross, Bernard Bioulac and Thomas Boraud *J Neurophysiol* 100:385-396, 2008. First published May 21, 2008; doi:10.1152/jn.90466.2008

# You might find this additional information useful...

This article cites 52 articles, 23 of which you can access free at: http://jn.physiology.org/cgi/content/full/100/1/385#BIBL

Updated information and services including high-resolution figures, can be found at: http://jn.physiology.org/cgi/content/full/100/1/385

Additional material and information about *Journal of Neurophysiology* can be found at: http://www.the-aps.org/publications/jn

This information is current as of July 15, 2008.

# Dynamic Changes in the Cortex-Basal Ganglia Network After Dopamine Depletion in the Rat

# Cyril Dejean, Christian E. Gross, Bernard Bioulac, and Thomas Boraud

Basal Gang, Laboratoire Mouvement, Adaptation, Cognition, Centre National de la Recherche Scientifique Unité Mixte de Recherche 5227, Université Victor Segalen Bordeaux 2 and Laboratoire Franco-Israélien de Neurophysiologie et Neurophysique des Systèmes, Bordeaux, France

Submitted 14 April 2008; accepted in final form 14 May 2008

Dejean C, Gross CE, Bioulac B, Boraud T. Dynamic changes in the cortex-basal ganglia network after dopamine depletion in the rat. JNeurophysiol 100: 385-396, 2008. First published May 21, 2008; doi:10.1152/jn.90466.2008. It is well established that parkinsonian syndrome is associated with alterations in the temporal pattern of neuronal activity and local field potentials in the basal ganglia (BG). An increase in synchronized oscillations has been observed in different BG nuclei in parkinsonian patients and animal models of this disease. However, the mechanisms underlying this phenomenon remain unclear. This study investigates the functional connectivity in the cortex-BG network of a rodent model of Parkinson's disease. Single neurons and local field potentials were simultaneously recorded in the motor cortex, the striatum, and the substantia nigra pars reticulata (SNr) of freely moving rats, and high-voltage spindles (HVSs) were used to compare signal transmission before and after dopaminergic depletion. It is shown that dopaminergic lesion results in a significant enhancement of oscillatory synchronization in the BG: the coherence between pairs of structures increased significantly and the percentage of oscillatory auto- and cross-correlograms. HVS episodes were also more numerous and longer. These changes were associated with a shortening of the latency of SNr response to cortical activation, from  $40.5 \pm 4.8$  to  $10.2 \pm 1.07$  ms. This result suggests that, in normal conditions, SNr neurons are likely to be driven by late inputs from the indirect pathway; however, after the lesion, their shorter latency also indicates an overactivation of the hyperdirect pathway. This study confirms that neuronal signal transmission is altered in the BG after dopamine depletion but also provides qualitative evidence for these changes at the cellular level.

# INTRODUCTION

The basal ganglia (BG) form a complex network that processes cortical information in the setting of motor control and learning (Graybiel et al. 1994). Classical models of Parkinson's disease (PD) make use of the discharge rate in the BG structures and predict that dopamine (DA) depletion can exert opposite effects on the direct and indirect BG pathways, which convey cortical information from the striatum to the output BG structures. This prediction has been validated in the striatum (Mallet et al. 2006) but not in the BG output structures (Murer et al. 1997; Robledo and Féger 1991; Taï et al. 2003; Wichmann et al. 1999). More recent studies in PD patients and in animal models of the disease showed synchronous oscillations between neurons and local field potentials (LFPs) in the cortex-BG network (Brown 2003; Hammond et al. 2007; Hutchi-

son et al. 2004). However, the changes in functional connectivity underlying the onset and transmission of pathological oscillations from the cortex to the BG remain poorly understood (Boraud et al. 2005).

The transmission of rhythmic cortical activity to the BG has been studied in urethane-anesthetized rats. With this preparation, the cortical discharge activity exhibits oscillations at  $\sim$ 1 Hz, which are reflected in the LFPs of the BG structures (Magill et al. 2004). Nevertheless, the discharge activity of the main BG output structure, the substantia nigra pars reticulata (SNr), is weakly correlated to these oscillations (Belluscio et al. 2003; Magill et al. 2004). However, in DA-depleted rats half of the SNr neurons exhibit a marked rhythmic activity which appears after the peak of cortical activity (Belluscio et al. 2003). Transmission from the cortex to the BG has also been studied in rats and monkeys using electrical stimulation of the motor cortex. Interestingly the dynamic response of BG output structures to cortical stimulation that has been observed in intact animals (Kolomiets et al. 2003; Maurice et al. 1999; Nambu et al. 2000) is both temporally altered and enhanced after DA depletion or blockade (Belluscio et al. 2007; Degos et al. 2005).

A third approach to the study of the transmission of cortical oscillations to the BG takes advantage of brief oscillatory events called high-voltage spindles (HVSs). HVSs are 5- to 13-Hz oscillations with a characteristic spike-and-wave shape. They occur spontaneously in awake rats when the animal is quietly resting. During HVS, neuronal activity and LFP are driven by cortical rhythm in all BG structures (Berke et al. 2004; Dejean et al. 2007; Deransart et al. 2003; Paz et al. 2005; Slaght et al. 2004). We showed that HVS makes it possible to study the functional connectivity of the BG (Dejean et al. 2007), without the disadvantages of the aforementioned techniques (anesthesia, electrical stimulation). The HVS approach described here was used to study the effect of DA depletion on the transmission of oscillations from the cortex to the BG in the unanaesthetized animal. For the purpose of this study, LFP and multiple single units were recorded simultaneously in the motor cortex, striatum, and SNr of awake and unrestrained rats before and after DA depletion.

Address for reprint requests and other correspondence: T. Boraud, Laboratoire Mouvement, Adaptation, Cognition, CNRS UMR 5227, Université Victor Segalen Bordeaux 2, 146 rue Leo Saignat, 33076 Bordeaux cedex, France (E-mail: tboraud@ u-bordeaux2.fr).

The costs of publication of this article were defrayed in part by the payment of page charges. The article must therefore be hereby marked "advertisement" in accordance with 18 U.S.C. Section 1734 solely to indicate this fact.

#### METHODS

#### Animals

Four male Wistar rats (350–400 g, Depré, Saint Doulchard, France) were kept under standard housing conditions at constant temperature (22  $\pm$  1°C), humidity (relative, 30%), and 12-hour light/dark cycles (daylight period 0800–2000 hours). Water was available ad libitum. Food intake was limited to 10–20 g/day to maintain constant animal weight. Animal care and surgery were consistent with the National Institute of Health *Guide for the Care and Use of Laboratory Animals* and the European community council directive of November 24 1986 (86/609/EEC) and was approved by the Comité Ethique de la Région Aquitaine.

#### Head stage

A custom head stage was designed for the purposes of this experiment to enable signals to be recorded simultaneously from the motor cortex anteroposterior (AP): +1.2 to +2.2 mm, mediolateral (ML): 1.5-2.5 mm, depth (D): 1.5-2.5 mm, the dorsal striatum (AP: +0.5 to -0.5 mm, ML: 3-4 mm, D: 3.5-5 mm) and the SNr (AD: -5.3 to -5.8 mm, ML: 1.8-2.7 mm, D: 7.5-8.5 mm). Details of the device's design and of the implantation surgery can be found in a previous publication (Dejean et al. 2007). To enable the required lesion of the midbrain dopaminergic neuron to be carried out, the head stage was equipped with a 28-gauge stainless steel cannula guide (Plastic One, Roanoke, VA). According to a stereotaxic atlas (Paxinos and Watson 1998), the guide was placed directly above the medial forebrain bundle that contains the nigrostriatal dopaminergic fibers (-2.8 mm AP and +2 mm ML). The cannula length was adjusted so that once it had been inserted into the guide, its tip was positioned in the upper third of the medial forebrain bundle (D: -8.4 mm). The lesioning procedure is described below.

# Surgery

The rats were operated under xylazine (60 mg/kg, ip; Rompun, Bayer, Germany) and ketamine (100 mg/kg, ip; Virbac, Carros, France) anesthesia. Using a stereotaxic frame (Kopf), recording targets were located, above which holes were drilled in the skull. The head stage was lowered, and the holes were filled with petroleum jelly (Vaseline, Gifrer Barbezat, Decines, France). The head stage was attached to the animal's skull with glue (Superbond, Sun Medical), dental cement (DentalonPlus, Heraeus Kulzer, Hanau, Germany), and stainless steel screws. Before the end of anesthesia, electrophysiological activities were recorded to make fine adjustments of the electrode positions when recorded signals did not agree with the characteristics of the targeted structures. The animals were given ketoprofen (ketofen, 2 mg/kg, sc; Merial, Lyon, France) after surgery, and again 24 h later for pain relief. The animals were allowed to recover for 7 days before the first recording session.

# Data acquisition

Daily recordings ran for 1 h in a circular arena (40 cm diam) during which physiological and behavioral activities were simultaneously recorded. Neural signals were preamplified 25 times (MiniHeadStage, AlphaOmega Engineering, Nazareth Illit, Israel) and amplified by a multichannel processor and digitized at a rate of 50 KHz (MCP, AlphaOmega Engineering). The raw signal was stored for further analysis at a lower rate of 12.5 KHz (AlphaMAP, AlphaOmega Engineering). In parallel, it was filtered (300 Hz to 3 KHz) for on-line spike discrimination using a template matching procedure (Multi Spike Discriminator, AlphaOmega Engineering). Discriminated spikes were stored synchronously with the raw signals. The animal's movements were recorded simultaneously by a video tracking system

(VTS, Plexon). Their position and the video recording were sampled at 30 Hz and stored separately from the neural data using video capture software (Cineplex, Plexon). Neural and behavioral signal recordings were triggered simultaneously, and the exact time of each position and video frame was sent to the AlphaMAP and stored in the neural data files for off-line synchronization.

At the end of the animals' recovery period, after surgical implantation of the head stages, recordings were made under normal conditions for 2 wk. The nigrostriatal fibers were lesioned, and recordings were again made under the same conditions for a period of 3 wk.

# 6-OHDA unilateral lesion procedure

One hour before 6-OHDA injection, the animals were pretreated with intraperitoneal injections of desipramine (0.4% solution, 25 mg/kg, Sigma-Aldrich France, Lyon, France) and pargyline (0.1% solution, 5 mg/kg, Sigma-Aldrich France). Desipramine is used to protect the noradrenaline neurons from 6-OHDA, and pargyline potentiates the efficacy of 6-OHDA by inhibiting monoamine oxydase (Dunnett 1983). The animals were anesthetized with isoflurane gas (induction at 4% and then 2%) for the duration of the 6-OHDA injection. The injection cannula was inserted through the guide mounted on the head stage, and a Hamilton syringe was used to inject 6-OHDA into the medial forebrain bundle (8  $\mu$ g in 1  $\mu$ l of sterile water at a rate of 0.5  $\mu$ l/min). After the injection had been completed, the syringe was left in place for 5 additional min to prevent the liquid from flowing back up the guide.

#### Histology

After the final recording, the rats were given a lethal dose of pentobarbital (Pentobarbital Sodique, CEVA, Libourne, France). Immediately after the injection, electrical microlesions (30  $\mu$ A, 10 s) were induced by passing an anodal current through one electrode at each recording site. The brain was quickly removed and frozen in an isopentane bath at  $-80^{\circ}$ C for histological analysis. Coronal brain sections (20  $\mu$ m) were cut and those encompassing the motor cortex, striatum, and SNr were mounted on slides for electrode placement verifications. These slices were stained with cresyl violet for structural identification. The recording tracks and sites were established by observing the marks left by the cannulae and electrolesions (Fig. 1A).

The extent of the SNc lesion can be determined by measuring the relative amount of dopamine cell terminals in the striatum ipsilateral to the lesion compared with contralateral (Kunikowska and Jenner 2001). Dopamine transporters are present at the membrane of nigrostriatal dopamine cell terminals and give a indirect measure of the amount of SNc dopaminergic cells projecting to the striatum. Dopamine transporter binding procedure was performed as described previously (Bezard et al. 2001). After purification, [125I](E)-N-(3-iodoprop-2-enyl)-2 $\beta$ -carboxymethyl-3 $\beta$ -(4'-methylphenyl) nortropane (PE2I) was obtained in a no-carrier-added form with a specific activity of 2,000 Ci/mmol and stored in ethanol at -20°C, a temperature at which it remains stable for 1 mo. Sections were incubated for 90 min at 25°C with 100 pM [125I] PE2I in pH 7.4 phosphate buffer (in mM: 10.14 NaH<sub>2</sub>PO<sub>4</sub>, 137 NaCl, 2.7 KCl, and 1.76 KH<sub>2</sub>PO<sub>4</sub>). After incubation, all sections were washed twice for 20 min in phosphate buffer at 4°C and dried at room temperature. They were exposed to  $\beta$  radiationsensitive film (Hyperfilm  $\beta$ -max, GE Healthcare, Buckingamshire, UK) in X-ray cassettes, for 7 days, for autoradiographic assessment of the radioactivity bound to regions of interest. The optical density was measured with an image analysis system (Densirag V. D2.00, Biocom, Les Ulis, France) and averaged for each right and left striatum in each animal.

#### Signal processing

BEHAVIORAL ANALYSIS. Off-line discrimination of movement and rest episodes was carried out using Cineplex Markup software

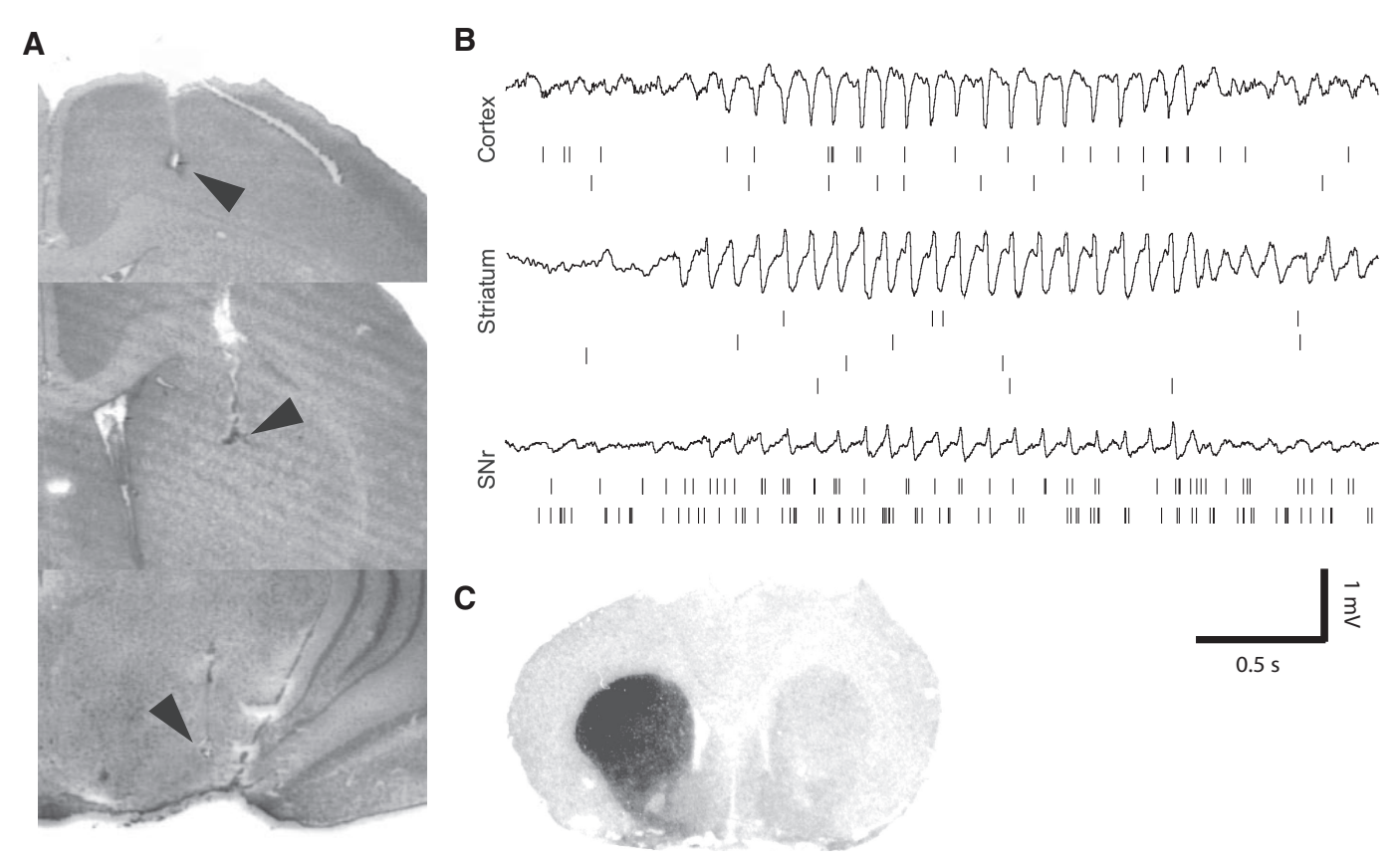


FIG. 1. Recording sites. A: coronal sections stained with cresyl violet at the level of recording sites in motor cortex (top), striatum (middle), and substantia nigra pars reticulata (SNr; bottom). Arrows show electrolytic microlesion locations. The 3 slices were taken from the same rat. B: electrophysiological activities simultaneously recorded in motor cortex (top), striatum (middle), and SNr (bottom) in the same rat as in B. The unbroken lines represent the local field potential. Below each recording, the vertical bars represent the spike trains of 2 neurons in the cortex, 4 neurons in the striatum, and 2 neurons in the SNr, respectively. C: autoradiography of a coronal section of the forebrain showing [1251](E)-N-(3-iodoprop-2-enyl)-2 $\beta$ -carboxymethyl-3 $\beta$ -(4'-methylphenyl) nortropane (PE2I) binding dopamine transporters in the striatum. The striatum ipsilateral to the lesioned hemisphere (right) shows very low dopamine transporters density.

(Plexon, Littleton, MA). The choice of the motor parameter to measure to asses the impact of the lesion on the animals' behavior was done in favor of locomotor activity. Locomotor activity has been shown recently to be decreased in rats bearing unilateral dopaminergic lesion (Steiner and Kitai 2001). Self-induced locomotor activity fits one important constraint of this study: to record physiological parameters in the unrestrained animal. For that reason we ruled out both the stepping test (Olsson et al. 1995) and drug-induced rotation tests.

Movement episodes consisted of periods during which the animal was moving (with the exception of grooming and rearing episodes). Basal locomotor activity was characterized by the average speed and SD (cm/s) during a typical rest episode for each rat. A threshold was defined as the upper confidence limit of the mean (see Statistical analyses). The animal was considered to be active when its instantaneous speed exceeded this threshold for >0.5 s. Rearing and grooming episodes were sorted manually using Cineplex Markup. The animals' locomotor activity was influenced by habituation to the environment. As expected, the prominent exploratory behavior observed during the first exposures of the animal to the recording chamber was decreased after a few days. To avoid confusion between the effect of lesion and habituation on locomotor activity, this study only considered data collected after the habituation phase for the behavioral analysis (Fig. S1)<sup>1</sup> Grooming episodes were automatically excluded because of the high incidence of mechanical artifacts on the simultaneous electrophysiological recordings. Rearing was present during the first days of the control period but quickly disappeared, as

the animal became accustomed to the recording chamber. For these reasons, rearing data are not discussed in this paper.

Analysis of the animals' specific behavioral patterns during HVS episodes showed that they were awake and resting quietly while remaining responsive to tactile, auditory, and visual stimuli. Neither whisker twitching movements nor tremors were observed during HVS before or after the lesion of the dopaminergic cells in the midbrain.

SPIKE DISCRIMINATION. The striatum contains several types of neuron, among which the medium spiny cells are the only output neurons. In this study, only putative medium spiny neurons (MSNs) discriminated according to shape and frequency criteria are described. Cells with a mean hyperpolarization duration >300  $\mu$ s and a firing rate <2 spikes/s (n=53) were classified as MSNs (Berke et al. 2004). Cells with a mean valley duration <300  $\mu$ s and a firing rate >1 spike/s were classified as interneuron-like neurons. Cells not satisfying one of these two conditions were rejected. Very few interneurons (n=3) were recorded during this study. As a consequence, results related to them are not presented here. All striatal neurons with waveform valleys <300  $\mu$ s and mean discharge rates under 1 spike/s were rejected.

At the depth of 1.5–2.5 mm at which neurons have been recorded in this study, the cortex contains interneurons and pyramidal neurons (not necessarily sending axons in the pyramidal tract). Both types were discriminated using a time criterion (Bartho et al. 2004). Cells presenting a peak valley duration >500  $\mu$ s were classified as putative pyramidal neurons (n=62). Other cells were classified as putative interneurons (n=2). Only pyramidal projection neurons were considered in this study. Corticostriatal neurons only represent a subset of

<sup>&</sup>lt;sup>1</sup> The online version of this article contains supplemental data.

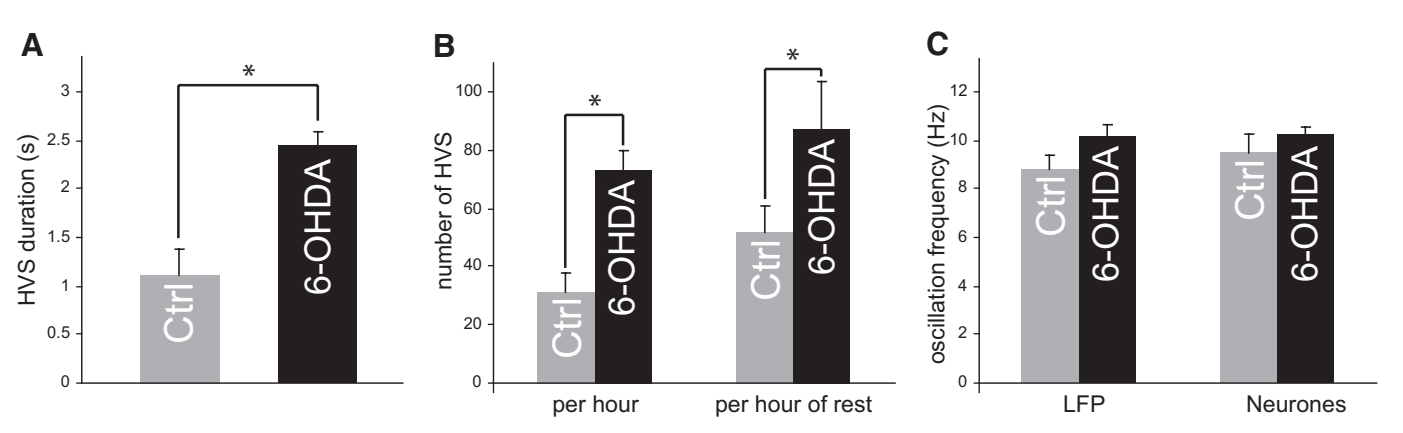


FIG. 2. Influence of the 6-OHDA lesion on high-voltage spindles (HVSs). A: duration of HVS. B: number of HVSs per hour of recording and per hour of rest. C: oscillation frequency during HVS for local field potentials (LFP) and neuron autocorrelograms. Gray bars, control condition; Black bars, after 6-0HDA. \*Significant difference between values under control and lesioned conditions as assessed with a paired t-test, except for the neuron frequency for which a t-test was used. The duration and number of HVSs are significantly increased after dopamine (DA) depletion, whereas there is no change in the oscillation frequency of LFP and neurons.

projection neurons. The setup and recording procedure described here does not allow connectivity tests to be performed, such as antidromic stimulation or marker tracing, to detect whether neurons were actually sending axons to the striatum. It was assumed that part of the recorded cortical neurons were putative corticostriatal neurons. Moreover, simultaneous multiple single-unit recordings showed that projecting neurons (thus including corticostriatal) fire synchronously in a short time window during HVS (Kandel and Buzsáki 1997). Therefore in our recordings, the overall firing time of cortical neurons is likely to be representative of the corticostriatal population itself.

The SNr contains a majority GABAergic neurons generating brief action potentials at a sustained firing rate and a few dopaminergic neurons, which when recorded extracellularly have been described as firing polyphasic long action potentials >1.5 ms at a slow rate <8 Hz (Hyland et al. 2002). Here the entire population of recorded neurons (n=76) presented short biphasic extracellular action potentials (ranging from 0.81 to 1.14 ms) with a rather high firing rate [18.4  $\pm$  1.9 (SE) Hz]. Thus they entered the study considered as putative GABAergic projection neurons.

HVS DISCRIMINATION. HVS's exhibit two main features, namely a spike and wave pattern and an oscillation frequency ranging between 5 and 13 Hz (Fig. 1B). Both criteria were used to detect the beginning and end of these episodes. For frequency criteria, a threshold on the instantaneous power spectral density (PSD) of local field potentials (LFPs) was used. LFPs were first filtered (1-200 Hz) using a secondorder band-pass Butterworth filter and down-sampled (500 Hz). For each structure, the PSD was computed every 100 ms using an overlapping sliding window with a length of 250 points (0.5 s). The instantaneous averaged PSD in the 5- to 13-Hz range was computed for each time step. Its value was deemed to have increased significantly when it passed the confidence limit (see Statistical analysis). Overthreshold time steps determined preliminary epochs. A pattern criterion was assessed manually. Preliminary epochs, within which the LFPs showed no typical spike and wave pattern, were rejected. Previous studies showed that HVS onset and offset could occasionally

be different in cortex and striatum (Berke et al. 2004). This lag can be attributed to the fact that onset and offset may vary across cortical locations (Polack et al. 2007; Shaw 2004). Since the cortical recording electrode was placed at a given location, the HVS could have been transmitted first from another cortical location to the striatum, thereby introducing an apparent onset delay. The same phenomenon could account for a delay in observed offsets. The analysis time frame was restricted to one oscillation cycle, where the cortex, striatum, and SNr were are all oscillating. To remove the lag-related bias, only those time intervals having overlapping candidate epochs were taken into account, using Neuroexplorer software (Nex Technologies, Littleton, MA).

HVS oscillation trough and peak markers were discriminated within HVS epochs using temporal and voltage criteria with a C++ homemade routine running under Matlab (The Mathworks, Natwick, MA). Cortical electrodes were placed around the border of layer V and VI (~1.5–2.5 mm below the surface) to record projection neurons. At this level, the earliest HVS spike component is negative (Kandel and Buzsáki 1997). For this reason, cortical LFP markers were positioned at the minimum voltage in the troughs. Because striatum and SNr spike components are positive, striatal and nigral markers were positioned at the maximum voltage in the peaks.

# Spectral characterization of LFP

The PSDs of LFPs were computed using fast Fourier transform (FFT) analysis and Welch method as spectral estimator with a sliding windows of 1,250 samples (2.5 s), over the frequency range from 0 to 500 Hz (0.39-Hz resolution). Histograms were smoothed using a three-point Gaussian process.

Coherence was computed using the expression

$$Coherence_{ij} = \frac{P_{ij} \times P_{ji}}{P_{ii} \times P_{ji}}$$

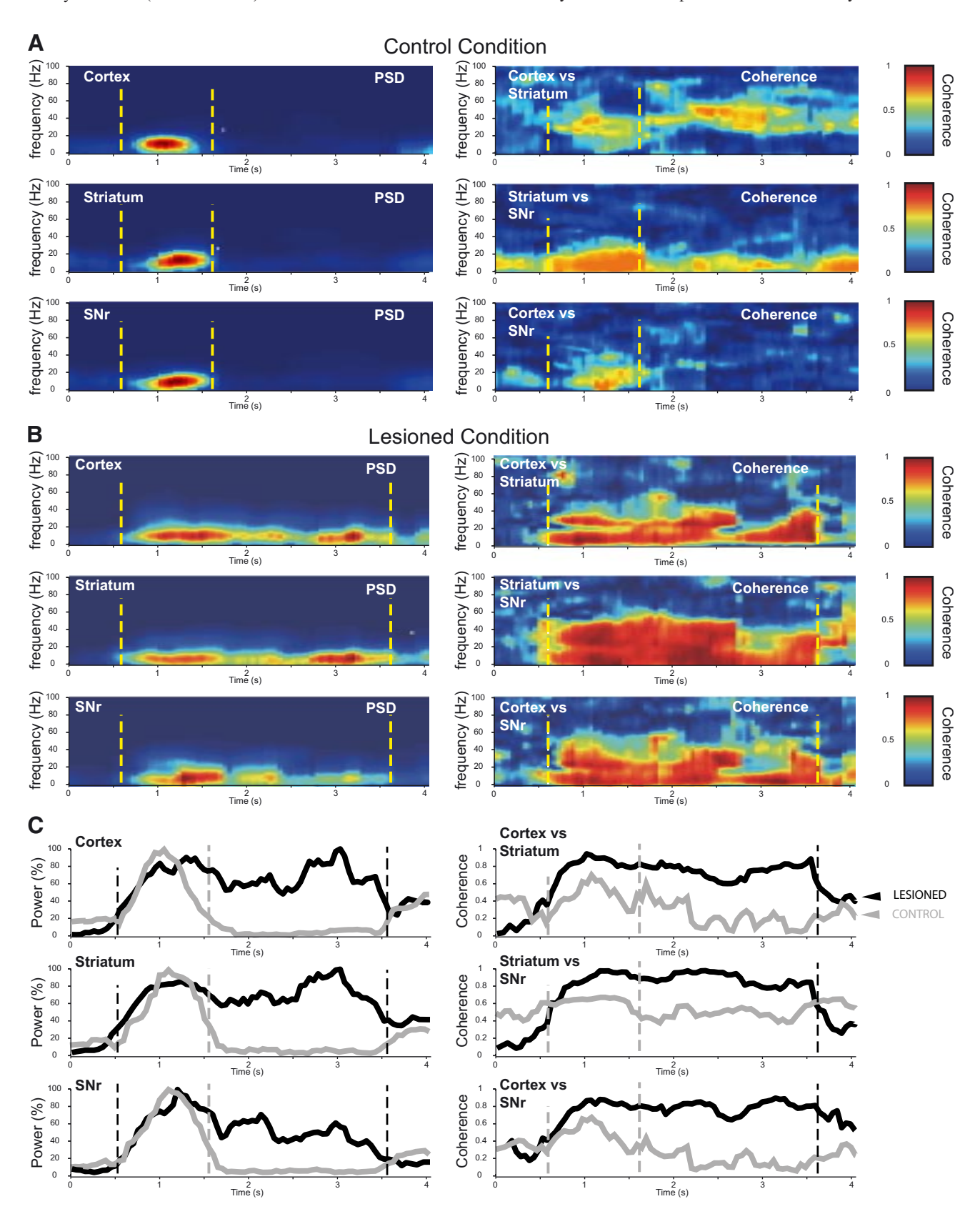
where P is the average of the squares of the LFP spectra i and j. These

FIG. 3. Only HVS discrimination and spectral analysis of LFPs during HVSs before and after DA depletion. A: example of an HVS under control conditions. Left: power spectral density (PSD) of simultaneously recorded LFPs as a function of time. Yellow dashed lines mark the beginning and the end of the HVS. The scale of relative power is in arbitrary units and is plotted in pseudocolors: blue is the minimum and red is the maximum. From top to bottom: power in the 0-to 100-Hz range of LFP recorded in the cortex, striatum, and SNr. In this example, the LFP sampling rate was 500 Hz, and the PSD was computed every 100 ms with a 250-point overlapping sliding window (0.5 s). Right: coherence as a function of time between each pair of LFPs shown on the left. The coherence value is plotted in pseudocolors (scale on the right). From top to bottom: coherence in the 0- to 100-Hz range between LFPs recorded in the cortex and striatum (top), striatum and SNr (middle), and cortex and SNr (bottom). B: example of an HVS after DA depletion in the same animal. The figures are organized in the same manner as for A. C: PSD and coherence from the previous examples are averaged over the 5- to 13-Hz frequency band. Gray line, control condition; Black line, after DA depletion. Left: PSD as a function of time. The PSD is scaled to the maximum value observed in the display window. The 3 sets of curves correspond to the 3 PSD images shown in A. Right: coherence as a function of time. The 3 sets of curves correspond to the 3 coherence images shown in A.

spectra were computed using the same method as described above (unless otherwise stated). Comparisons between coherence histograms computed during rest, movement, and HVS episodes were made using a one-way ANOVA (with P=0.05).

# Characterization of spike trains

Cross-correlograms were computed using a bin size of 2 ms with 50 randomly chosen action potentials to avoid analytic bias related to



J Neurophysiol • VOL 100 • JULY 2008 • www.jn.org

potential differences in sample size, especially when comparing before and after the lesion. Cross-correlogram PSDs were computed by FFT, using sliding windows of 256 samples (1.28 s) over the frequency range 0–200 Hz, yielding a resolution of 0.8 Hz. Histograms were smoothed using a three-point gaussian process. The confidence limit (CL) of the PSD histograms was computed over the 3- to 50-Hz range (see *Statistical analysis*), and autocorrelograms and cross-correlograms were considered oscillatory if any PSD value in the spectral window from 5 to 13 Hz passed the CL (with P < 0.01).

#### Time lag distributions

Peri-event histograms of the discharge activity of single neurons and of the next cortical LFP markers were constructed, using the HVS cortical marker as a trigger  $(t_0)$ , over a time frame of 100 ms before and after  $t_0$ . For the purposes of graphical representation, a 2-ms bin size and a three-point gaussian smoothing algorithm were used. For this analysis only, triggers and spike trains that occurred >50 times in the HVS epochs were considered. A peak was considered significant if it exceeded the upper CL (see *Statistical analysis*), and a trough was considered significant if its value was below the lower CL. The presence of a significant peak and/or trough was used as a criterion in defining a neuron to be "HVS driven." For the HVS driven neurons, peak and trough times were averaged to construct population time lag distributions in the time range of 50 ms before and 140 ms after cortical LFP marker.

# Phase relationship

To determine the phase relationship between neurons and cortical LFPs following the method used by Klausberger et al. (2003), we used a Matlab algorithm (see HVS discrimination section above) to detect the troughs of HVS. Each spike was assigned to a phase between the troughs n and n + 1 given that the peak of LFPs was arbitrarily assigned the angle value 0°. The circular space was divided into 100 bins of equal size giving a resolution of 3.6°. The significance of the phase relationship was analyzed using the Rayleigh test for directional data (Fisher 1993). This tests the hypothesis that spike phases are uniformly distributed along the circular space (0-360°). For each spike train, this test was carried on 50 randomly chosen action potentials to test samples of the same size and avoid analytic bias related to differences in sample size. The preferred phase (i.e., phase represented by the highest number of spikes) was collected to construct and compare the phase distributions for neurons of each structure before and after dopamine depletion. This phase analysis of neuronal spike trains showed that the neurons that presented a significant bias toward a preferred phase of cortical LFPs were also the ones that were defined as HVS driven by the time lag analysis (previous section). This shows that firing rate of neurons selected for this study had no influence on their oscillatory behavior.

#### Statistical analysis

Statistical analyses were performed with Sigma Stat software (Version 2.03, SPSS, Chicago, IL) and GraphPad Prism (version 4.00, GraphPad Software, San Diego CA). A probability level of 5% (P < 0.05) was considered significant. Variables are presented in the following form: means  $\pm$  SE.

CLs were computed as  $CL = mean \pm 3$  SD. Comparisons between mean locomotor activity were made using a two-way ANOVA (factor 1: selected rat; factor 2: control/lesion) to assess the influence of the extent of the lesion in each rat. HVS duration and number and LFP oscillation frequencies were assessed using a paired t-test (normal and dopamine-depleted animals). Coherence was analyzed using a two-way ANOVA (factor 1: selected rat; factor 2: pair of structures) followed by post hoc multiple comparisons using the Holm-Sidak method and a paired t-test to assess the influence of the lesion on the

level of coherence. Oscillatory AC and CC percentages were analyzed using  $\chi^2$  tests (normal and dopamine depleted). Firing rates during and outside HVS episodes were compared using a Mann-Whitney rank sum test. AC mean oscillation frequencies were compared using a *t*-test (normal and dopamine depleted). Firing rates presented nonnormal distributions and were therefore analyzed using a nonparametric test: a Mann-Whitney rank sum (normal and dopamine depleted) and a one-way ANOVA on ranks (total, oscillatory, and nonoscillatory), followed by post hoc multiple comparisons using Dunn's method. Time lags between neuron firing peaks and LFP peaks presented non-normal distributions and unequal variances. They were therefore analyzed using a Mann-Whitney rank sum test (normal and dopamine depleted).

The comparison of phase distributions in the circular space for control and lesion condition was done using the Watson U2 test (Fisher 1993).

The locomotor activity is expressed as a percentage of the time spent moving under control conditions. ACs and CCs are presented as a percentage of the total AC and CC, respectively.

#### RESULTS

Extent of striatonigral lesion and behavioral impairment

In the striatum ipsilateral to the lesion, the optical density for the striatum decreased by an average of  $78.2 \pm 6.9\%$  (range, 68.5–90.9) compared with the contralateral hemisphere (see example on Fig. 1*C*). Under control conditions, the animals spent  $20.6 \pm 0.8\%$  of their time moving (range: 13.7–30.1%). Three weeks after the lesion was processed, the percentage of time spent moving decreased significantly, by an average of >50%, to reach  $9.5 \pm 0.5\%$ . The lesion was the significant factor influencing the drop in locomotor activity explaining 73% of the variance, whereas the animal only accounted for 14% [2-way ANOVA, F(1,19) = 123.78, P < 0.05 and F(19,19) = 1.41 P = 0.23, respectively, with no interaction]. Therefore the lesion procedure induced a marked homogeneous behavioral impairment in all the animals.

# Effects of dopaminergic depletion on HVS features

Under normal conditions, the mean duration of a HVS was  $1.1 \pm 0.3$  s (Fig. 2*A*), and the mean number of episodes was  $30.7 \pm 6.3$  per hour and  $52.0 \pm 8.3$  per hour of rest (Fig. 2*B*). The HVS mean frequency was  $8.8 \pm 0.4$  Hz, with a frequency range extending from 5 to 13 Hz (Fig. 2*C*). During HVS, the coherence in the range 5–13 Hz between the different pairs of LFPs was  $0.47 \pm 0.03$  in cortex-striatum pairs,  $0.30 \pm 0.03$  in striatum-SNr pairs, and  $0.26 \pm 0.04$  in cortex-SNr pairs (Figs. 3 and 4), such that cortex-striatum coherence was significantly higher than in the case of striatum-SNr and cortex-SNr. The latter was not significantly different [2-way ANOVA, selected-rat factor: F(3,12) = 1.54 P = 0.56 and pair-of-structures factor: F(2,12) = 5.42, P < 0.05; Holm-Sidak post hoc comparison method: P < 0.05, P < 0.05 and P = 0.57 for cortex-striatum, striatum-SNr, and cortex-SNr pairs respectively].

Under parkinsonian conditions (as shown for example in Fig. 3, B and C), the mean duration of HVS episodes increased significantly (Fig. 2A;  $2.6 \pm 0.2$  s; paired t-test, P < 0.05) as did the number of episodes per hour and per hour of rest (Fig. 2B: respectively,  $72.2 \pm 4.7$  and  $86.7 \pm 3.5$ , paired t-test: P < 0.05 and P < 0.05). The HVS mean frequency was not significantly modified (Fig. 2C;  $9.6 \pm 0.5$  Hz; range, 5–14 Hz).

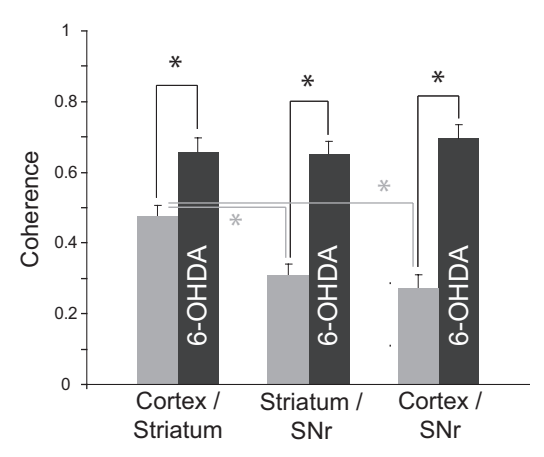


FIG. 4. Influence of the 6-OHDA lesion on the coherence in the 5- to 13-Hz range. Under control conditions (gray bars), coherence is higher in the corticostriatal pairs of LFPs. After 6-OHDA lesion (black bars), the coherence is significantly increased for each pair, and there are no longer any significant differences observed between pairs. \*Significant difference between coherence values (1-way ANOVA and Bonferroni post hoc).

As shown in the example of Fig. 3C, the coherence values were also increased (Fig. 4) and reached  $0.65 \pm 0.04$  in cortex-striatum pairs,  $0.64 \pm 0.03$  in striatum-SNr pairs, and  $0.69 \pm 0.04$  in cortex-SNr pairs (paired t-test: P < 0.05 for each pair). We also noticed an increase in coherence in the beta band (15–30 Hz) between each pair of structures, although the spectral power around 20 Hz was negligible compared with that between 8 and 13 Hz (Fig. 3, A and B). The increased duration of HVS episodes could affect the overall coherence level by improving resolvability of the signal. However, when computed as a function of time, coherence still shows an increase in the lesion condition; therefore the length of time intervals has no influence on the level of coherence.

#### Dopaminergic depletion enhances neuronal rhythmic firing

Under normal conditions, 25 neurons were recorded in the motor cortex, 17 MSNs in the striatum, and 31 neurons in the SNr. Firing rates during HVS were  $4.1 \pm 1.3$  spikes/s in the cortex,  $0.8 \pm 0.2$  in the striatum, and  $18.4 \pm 1.9$  in the SNr (Fig. 5). On average, no significant changes were observed between HVS episodes and other epochs of our recordings (paired t-test: P = 0.976, P = 0.759, and P = 0.489, respectively). During HVS under normal conditions, the average oscillation frequency of the neuron autocorrelograms (Fig. 2C) was not significantly different from that observed in the LFP (t-test:  $9.5 \pm 0.3$  Hz, with a range extending from 6.1 to 11.4, P = 0.209). The proportion of oscillatory autocorrelograms was 45% in the cortex, 30% in the striatum, and 55% in the SNr (Fig. 6, A-C). The proportion of oscillatory intrastructure cross-correlograms was 62% in the cortex, 35% in the striatum, and 60% in the SNr (Fig. 6, A, B, and D). Interstructure cross-correlogram analysis showed that 22% of cortex-striatum pairs of neurons, 51% of striatum-SNr pairs, and 53% of cortex-SNr pairs were oscillatory. As expected, auto- and cross-correlogram percentages were significantly higher during HVS than during the other recording periods, in which the number of significant synchronizations and oscillations hardly reached 5% ( $\chi^2$  test: P < 0.05, data not shown).

Under parkinsonian conditions, 37 neurons were recorded in the motor cortex, 36 MSNs in the striatum, and 46 neurons in the SNr. The firing rate (Fig. 5) in the cortex and striatum did not change (2.5  $\pm$  0.4 spikes/s, Mann-Whitney rank sum test: P = 0.154; 0.8  $\pm$  0.1 spike/s, Mann-Whitney rank sum test: P = 0.851, respectively), whereas it increased significantly in the SNr (25.4  $\pm$  1.9, Mann-Whitney rank sum test: P < 0.05). On average, no significant changes in firing rate were observed between the HVS episodes and other epochs of our recordings (Mann-Whitney rank sum test: P = 0.705, P = 0.850, and P =0.930, respectively). The percentage of oscillatory autocorrelograms increased significantly to reach 76% in the cortex, 58% in the striatum, and 89% in the SNr (Fig. 6, A-C). The average oscillation frequency observed in these autocorrelograms (Fig. 2C) did not significantly differ from that observed under normal conditions (10.3  $\pm$  0.3 Hz with a range extending from 7.4 to 13.1, t-test: P = 0.129). The percentage of oscillatory intrastructure cross-correlograms increased significantly, reaching 86% in the cortex, 78% in the striatum, and 81% in the SNr ( $\chi^2$  test: P < 0.05, P < 0.05, and P < 0.05,

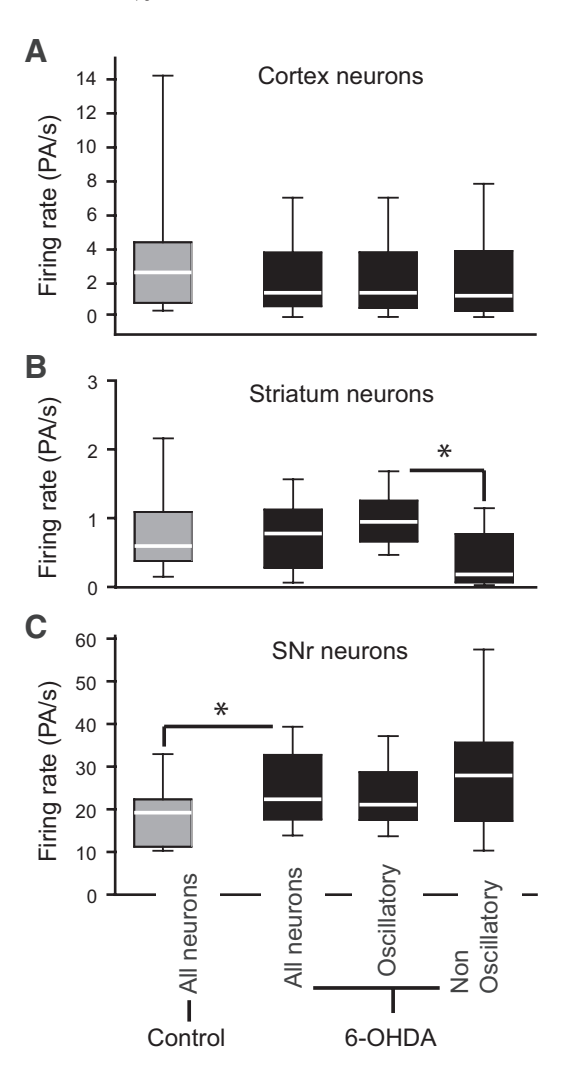


FIG. 5. Changes in firing rates after 6-OHDA lesion. Box plot of the distributions of firing rates of neurons recorded under control and parkinsonian conditions. Under parkinsonian conditions, distributions for neurons presenting oscillatory and nonoscillatory autocorrelograms (for display examples, see Fig. 6) have been added to the display. A: cortical neurons. B: striatal neurons. C: nigral neurons. \*Significant difference between distributions, as assessed using one-way ANOVA on ranks (total, oscillatory, and nonoscillatory) followed by a post hoc multiple comparison using Dunn's method.

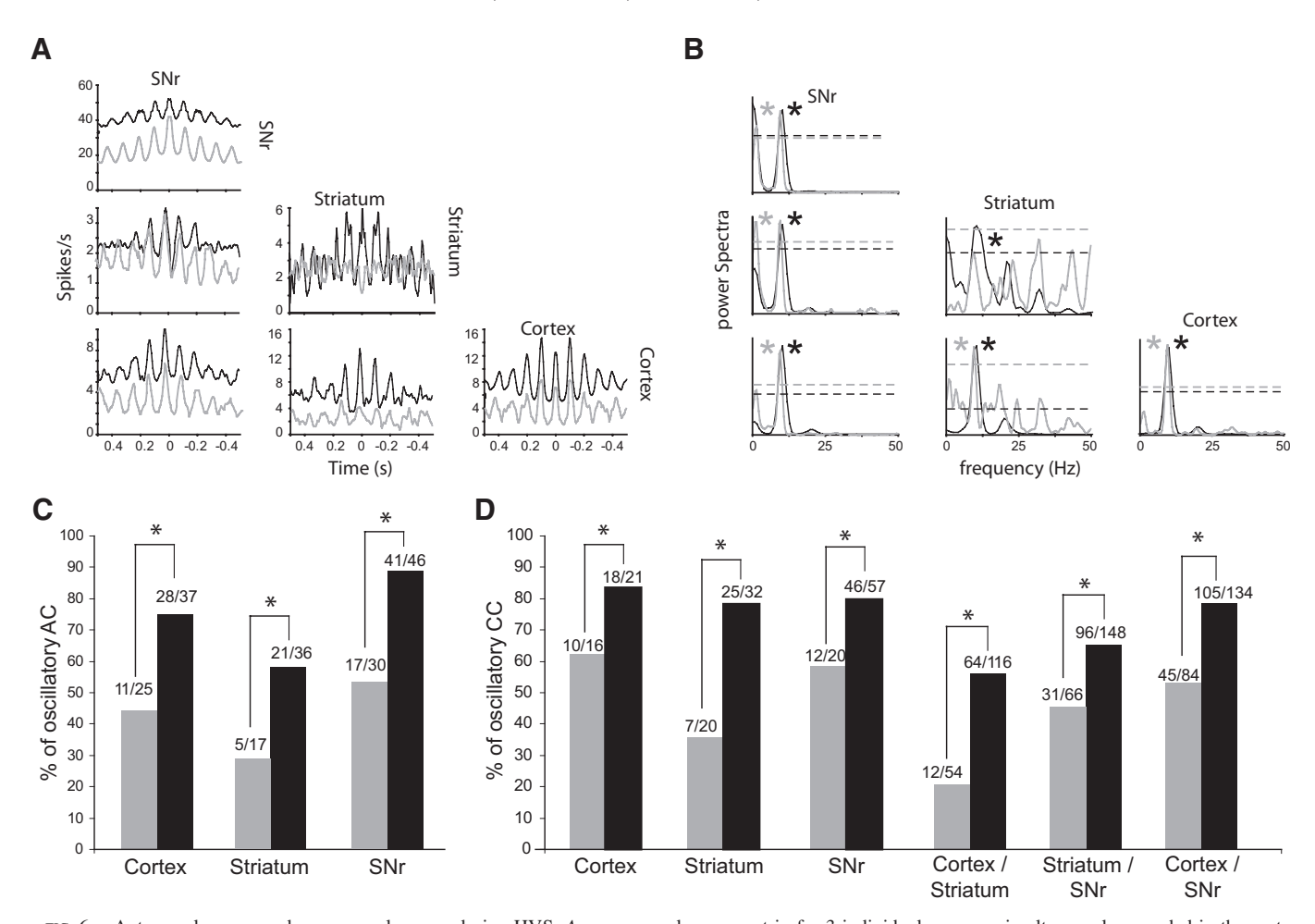


FIG. 6. Autocorrelograms and cross-correlograms during HVS. A: cross-correlogram matrix for 3 individual neurons simultaneously recorded in the motor cortex, striatum, and SNr. Gray lines, 3 neurons recorded under control conditions; black lines, 3 neurons recorded in the same rat under lesioned conditions. The matrix of cross-correlogram is built as follows. From *top* to *bottom*: SNr, striatum, and cortex. From *left* to *right*: SNr, striatum, and cortex. Each of the 9 points of the matrix represents the cross-correlation function of the 2 neurons of the corresponding row and column. The columns give the trigger neuron and the rows give the correlated neuron. The diagonal displays particular cross-correlograms called autocorrelograms in which the reference neuron is also the tested neuron and the other points of the matrix represent the cross-correlograms. Note that a cross-correlation matrix is symmetrical; as a consequence, the cross-correlograms on the *top right* are identical to the cross-correlograms on the *bottom left*. To lighten the figure, the redundant data on the *top right* are not shown. B: PSDs of the cross-correlograms shown in A. The dashed lines represent the significance threshold of the power peak (P < 0.05). \*Significant peak. Color code is the same as in A. C: percentage of oscillatory autocorrelograms (ACs) of neurons recorded in the cortex, striatum, and SNr. D: percentage of oscillatory cross-correlograms (CC) of pairs of simultaneously recorded neurons. For C and D, \*significant difference between values under control and lesioned conditions, as assessed with a t-test. DA depletion significantly increased the percentage of oscillatory neurons and that of oscillatory synchronization between neurons.

respectively). Interestingly, striatal neurons that exhibited oscillatory autocorrelograms presented a significantly higher firing rate than nonoscillatory neurons (Fig. 5B). Firing frequencies were  $1.1\pm0.2$  and  $0.4\pm0.1$  spike/s during HVS and outside HVS, respectively (Mann-Whitney rank sum test: P<0.05). This difference was not observed before the lesion (Mann-Whitney rank sum test: P=0.546; data not shown). The percentages of oscillatory extrastructure cross-correlograms were also enhanced by DA depletion for each pair of structures (Fig. 6D). They reached 55% for cortex-striatum pairs of neurons, 65% for striatum-SNr pairs, and 78% for cortex-SNr pairs ( $\chi^2$  test: P<0.05, P<0.05, and P<0.05, respectively).

Alteration of the temporal organization of neuron discharges in DA-depleted rats

As shown in the example of Fig. 7, A-C, examination of the peri-event histograms showed that a majority of neurons in

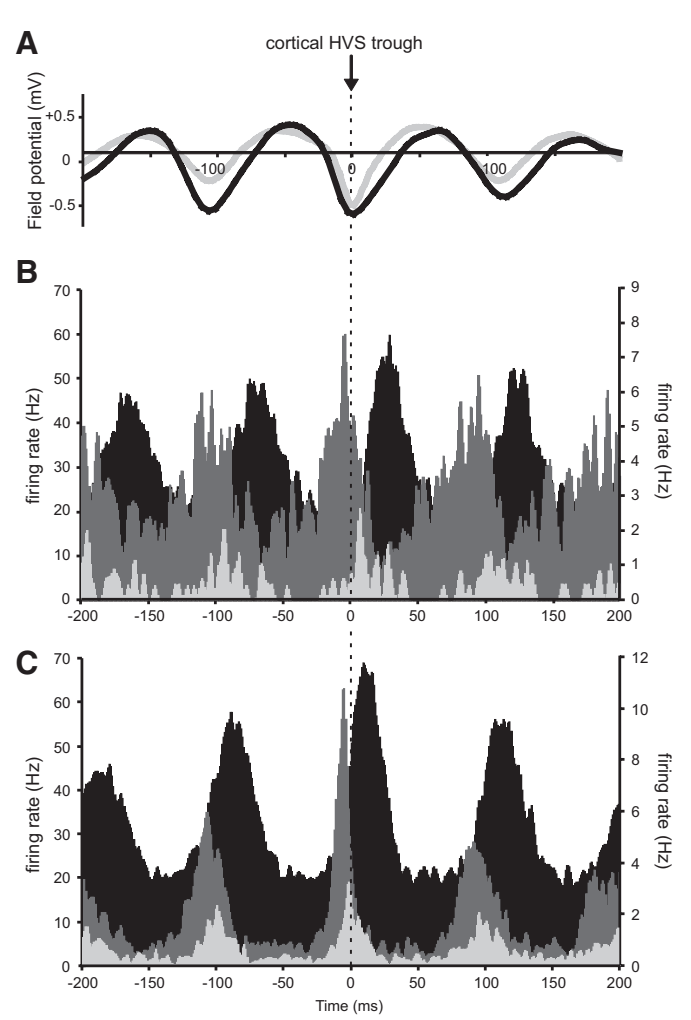
each structure was driven by the cortical rhythm during HVS, under both control conditions and after lesion of the nigrostriatal pathway (Table 1). The peri-event histograms allowed us to detect rhythmicity in the MSNs, which, as a consequence of their sparse firing activity, was not shown by the autocorrelation function.

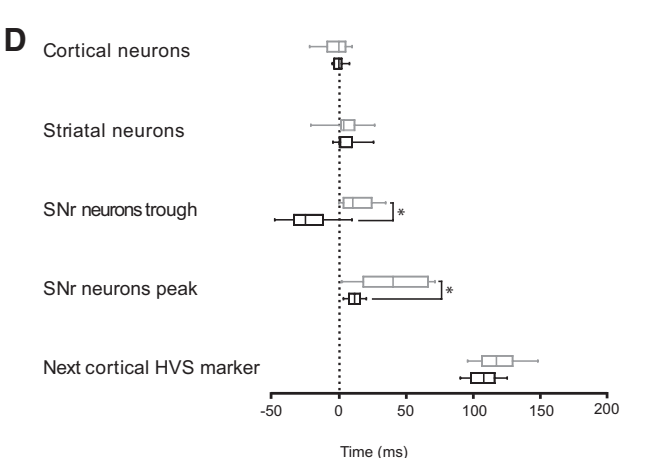
Under control conditions, when timed with respect to the cortical HVS marker, cortical firing peaked at  $-5.8 \pm 4.2$  ms, striatal activity peaked at  $3.2 \pm 3.9$  ms, the minimum of SNr activity occurred at  $15.6 \pm 3.9$  ms, and SNr activity peaked at  $40.5 \pm 4.8$  ms (Fig. 7D). In the cortex and striatum, these

TABLE 1.

	Cortex	%	Striatum	%	SNr	%
Control	16/25	64%	10/17	59%	17/30	57%
6-OHDA	27/37	72%	22/36	61%	40/46	74%

results are consistent with other studies of freely moving animals (Berke et al. 2004; Kandel and Buzsáki 1997). To the best of our knowledge, equivalent data have not been reported for SNr neurons. After DA depletion, the pattern of activation was significantly altered only in SNr: the minimum and maximum of SNr activity occurred respectively earlier at  $-24.3 \pm 4.4$  and  $10.2 \pm 1.07$  ms, respectively, with respect to the cortical HVS marker. Moreover, the percentage of SNr neurons exhibiting troughs significantly fell from 58% before the lesion to 34% afterward ( $\chi^2$  test, P < 0.05). In contrast, the percent-





age of SNr neurons exhibiting peaks significantly increased from 58 to 87% ( $\chi^2$  test, P < 0.05). No significant shifts were observed in the case of cortical and striatal neurons (Mann-Whitney rank sum test: P = 0.972 and P = 0.921, respectively). The period of the oscillations, computed with the intervals between the cortical HVS trough markers (Fig. 8, A and D), also did not change before and after the lesion (t-test, P = 0.740). This indicates that the firing peak shift observed in the SNr was not caused by a decrease in oscillation period.

# Alteration of the phase of neuron discharges in DA-depleted rats

The phase analysis showed that a majority of neurons displayed a bias toward a preferred phase of the cortical LFPs (Rayleigh test). Moreover, the population of oscillatory neurons matched exactly the population of 'HVS driven' neurons.

The SNr neuron phases are altered toward smaller values after the lesion with a significant shift from  $124 \pm 15$  to  $34 \pm 5^{\circ}$  (Watson U2 test, P < 0.05). On the contrary, the phases of cortical (control:  $-14 \pm 11^{\circ}$ ; lesion:  $-9 \pm 5^{\circ}$ ) and striatal neurons (control:  $8 \pm 12^{\circ}$ ; lesion:  $18 \pm 9^{\circ}$ ) action potentials remained stable (Fig. 8; Watson U2 test, P > 0.05).

#### DISCUSSION

In this study, we examined HVS to compare connectivity in the cortex-BG network before and after dopaminergic depletion. The main finding using this original approach is the demonstration that the temporal distribution of discharge activity in the network is altered after dopaminergic lesion: nigral neurons responded significantly earlier to cortical activation. Moreover, DA depletion induced an overall increase in synchronization in the network during HVS, and this effect was particularly pronounced in the case of striatal output neurons.

## DA depletion and locomotor impairment

In our study, the average level of striatal dopaminergic terminal loss was >68%. We observed both an increase in oscillatory activity during HVS and a decrease in locomotor activity. This is consistent with a recent study showing that akinesia and changes in the dynamic properties of BG neurons appear when striatum presents a decrease of >70% of dopaminergic terminals (Tseng et al. 2005). The decrease in motor activity (55%), observed 20 days after the lesion was intro-

FIG. 7. Temporal organization of neurons and LFP during HVS. A: perievent histogram triggered on LFP markers in the cortex (dotted line) for cortical LFPs recorded in the same rat under control conditions (gray line) and after dopaminergic depletion (black line). B: peri-event histogram triggered on LFP markers in the cortex (dotted line) for 3 neurons simultaneously recorded under control conditions. Dark gray bars, neuron in cortex; light gray bars, striatum; black bars, SNr. Left ordinal scale is for nigral neurons and right scale is for cortical and striatal neurons. C: peri-event histogram triggered on LFP markers in the cortex (dotted line) for 3 neuron spike trains simultaneously recorded after DA depletion (the neurons are different from those shown in B). Same color code as in A. Left ordinal scale is for nigral neurons and right scale is for cortical and striatal neurons. D: time lag distributions of neuronal activity and of the next cortical HVS marker under control (gray boxes) and lesioned conditions (black boxes). \*Significant difference between distributions before and after the lesion (Mann-Whitney rank sum test). DA depletion significantly shortens the latency of SNr neuron peaks and troughs, and this is not because of an alteration of the HVS period.

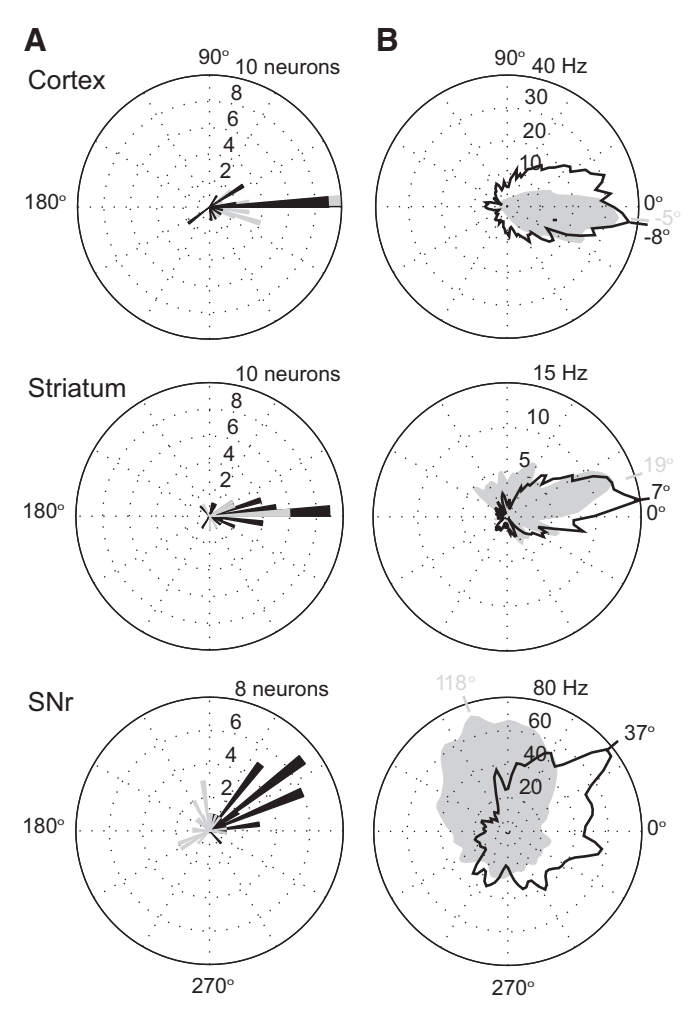


FIG. 8. Phase relationship between cortical, striatal, and SNr spikes and cortical LFPs. A: the polar plots summarize the distributions of the preferred phase of all oscillatory neurons in cortex (top), striatum (middle), and SNr (bottom) with regard to cortical LFPs (angle 0° corresponding to LFPs peak). Neurons recorded before the lesion are represented in gray and those recorded after the lesion are plotted in black. B: examples of firing as a function of phase for single neurons recorded before (gray) and after (after) the lesion. The firing rate scale indicates the average firing rate in hertz per bin (3.6°). Ticks and corresponding angle value on the outer cycle show the preferred phase of the neurons.

duced, is also consistent with a previous study (Steiner and Kitai 2001).

# DA depletion increases cortex-BG synchronization during HVS

We observed that neuronal oscillatory and synchronous activity is increased in all structures and most notably in the striatum. This increase is consistent with previous studies of the striatum (Tseng et al. 2001) and SNr (Belluscio et al. 2003) of anesthetized rats. In agreement with studies in the parkinsonian monkey (Goldberg et al. 2002; Nini et al. 1995), we also observed an increase in intracortical and intranigral neuronal synchronization. We have shown that the level of interstructure oscillatory synchronization in the BG increases, whichever pair of structures is considered, both in the HVS (5–13 Hz) and the beta band (15–30 Hz). This increase is particularly pronounced in pairs involving striatal neurons and is likely caused by the

enhancement of oscillations in a subpopulation of MSNs. On the whole, our observations related to HVS are in agreement with numerous publications, showing that synchronous oscillations are enhanced in the presence of parkinsonian conditions (Belluscio et al. 2003; Bergman et al. 1994; Meissner et al. 2005; Sharott et al. 2005). An alternate hypothesis has been evoked to explain increased synchronized oscillations in parkinsonian conditions. A popular one is the reverberating STN-GPe loop (Bevan et al. 2002); however, in our case, the shortening of the latency between cortical and SNr responses and of the phase of the SNr neuronal responses rendered this hypothesis very unlikely as far as HVSs are concerned. We nevertheless do not rule out that these mechanisms play a role in the stabilization and/or the generation of other type of oscillations.

# DA depletion increases the number and duration of HVSs

After DA depletion, HVS spindles are significantly longer and more numerous than under normal conditions, and the coherence between each pair of structures is increased. Our observations are consistent with previous studies, showing that alteration of the BG leads to modification in the occurrence of HVS, although they are not involved in their generation (Deransart et al. 1998). Indeed, the number and duration of HVS have been shown to be diminished by the injection of dopaminergic agonists inside the striatum (Deransart et al. 2000). The increase in number and duration of HVS observed after DA depletion is thus in line with previous observations by Deransart et al. (2000) and could be caused by the enhancement of oscillatory synchronization in the cortex-BG network, which we have shown is particularly pronounced in the striatum.

# DA depletion qualitatively changes the top-down transmission of information

Studies carried out in rats and monkeys have shown that frontal or prefrontal cortical stimulation can elicit complex responses in the BG output structures, the SNr, or the globus pallidus pars interna (Kolomiets et al. 2003; Maurice et al. 1999; Nambu et al. 2000). These authors have reported triphasic responses in the majority of SNr neurons characterized by an early excitation, followed by an inhibition and a late excitation. Each component of this response has been attributed to the activation of one of the three BG pathways with, in chronological order, the trans-subthalamic hyperdirect pathway (excitatory, between  $\sim$ 7 and  $\sim$ 16 ms), the *trans*-striatal direct pathway (inhibitory, between  $\sim 10$  and  $\sim 30$  ms), and the indirect pathways (excitatory, between  $\sim$ 25 and  $\sim$ 50 ms). With our approach, under normal conditions, the trough in SNr activity follows the cortical peak by 15.6 ms, and the SNr peak occurs 40.5 ms after the cortical peak. On the basis of these values, we have previously suggested that during HVS, SNr activity is driven by inputs from the direct and indirect pathways, but not by the hyperdirect pathway (Dejean et al. 2007).

After dopaminergic depletion, we observed two major phenomena: *I*) the SNr trough no longer seemed to be driven by the cortical rhythm, because this feature was no longer observable in more than third of the neurons and it also occurred 23.4 ms earlier than the cortical HVS; and *2*) the SNr firing peak occurred significantly earlier, i.e., its delay after the cortical

HVS marker decreased from 40.5 to 10.2 ms. The SNr peak thus occurs inside the time window of the electrically evoked responses mediated by the hyperdirect pathway (Kolomiets et al. 2003; Maurice et al. 1999; Nambu et al. 2000). However, the duration (40 ms) of the excitatory response observed after DA depletion suggests that this form of excitation is not only mediated by the hyperdirect pathway but is also merged with a late excitatory component likely caused by the activation of the indirect pathway. In conclusion, these alterations may be caused by a decrease in efficiency of the direct pathway, associated with an increase in that of the hyperdirect and indirect pathways. Numerous lines of evidence in the literature support this conclusion. On the one hand, a weakening of the direct pathway is in line with classical models of the pathophysiology of PD (Albin et al. 1989; DeLong 1990). This view has returned to the forefront of BG research with very recent studies using cortical stimulation in anesthetized animal. Indeed Mallet et al. (2006) have shown that DA depletion strongly depresses the response of striatonigral-direct-pathway neurons to cortical input. Moreover, two other groups showed a decrease of direct pathway influence on SNr neurons in both the unilateral 6-OHDA model used here (Belluscio et al. 2007) and an acute model of PD (Degos et al. 2005). On the other hand, it has been shown that DA depletion facilitates the transmission of cortical oscillations to the STN and the globus pallidus in the rat. It has been further suggested that both hyperdirect and indirect pathways were strengthened (Magill et al. 2001; Walters et al. 2007). Importantly, strengthening of the indirect pathway is also in agreement with classical models and has recently been shown by electrophysiological and anatomical studies in the striatum (Day et al. 2006; Mallet et al. 2006). These studies support the presence of an imbalance between striatonigral and striatopallidal neurons as stressed in the classic models. In this study, we observed that rhythmically driven MSNs showed significantly higher firing rates than nondriven units under parkinsonian conditions. Rhythmically driven and nondriven neurons could therefore correspond to striatopallidal and striatonigral MSNs, respectively.

We propose that the loss of striatal inhibition unmasks the earliest excitatory components, caused by the indirect pathway. In this study, we also observed a possible overexpression of the hyperdirect pathway in the SNr. The removal of direct inhibitory influence may leave a time window open for hyperdirect inputs, which were probably overshadowed by striatal inhibition under control conditions (Dejean et al. 2007).

### Striatal gating of oscillatory signals

As in previous studies, we showed that, despite the strong coherence observed between cortical and striatal LFPs (Mahon et al. 2001; Slaght et al. 2004; Stern et al. 1997), oscillations in the spiking activity of MSNs are weak (for a detailed discussion of this point see Berke et al. 2004; Dejean et al. 2007). This lack of oscillatory output can explain the discrepancy between the observed level of coherence between cortex and striatum and that between either striatum and SNr or cortex and SNr. However, after 6-OHDA lesion, these differences in coherence level disappeared. Moreover, the striatal MSNs show the greatest increase in oscillatory and synchronized firing behavior. Our results suggest that DA depletion facilitates the transmission of oscillations through the striatum. This

is consistent with recent theories of BG in which the striatum acts as a gate for information flowing toward downstream structures (Murer et al. 2002; O'Donnell 2003).

#### Conclusion

Among various symptoms, patients with Parkinson's disease present a strong impairment in the initiation of movement and a marked slowing of reaction times (Agid 1991). We have recently shown that the latter is correlated with a paradoxical shortening of the response latency of BG output neurons: in the MPTP monkey the neurons of the globus pallidus pars interna respond earlier to a "go-movement" stimulus (Leblois et al. 2006). These results provide an explanation for this finding by showing that it may rely on an alteration of the computation of information from the concurrent BG pathways.

#### ACKNOWLEDGMENTS

The authors thank Dr. Francois Gonon for helpful comments on the manuscript and S. Dovero and L. Cardoit for the histology. Dr. Martin Guthrie performed the final review of English spelling and grammar.

Present address of C. Dejean: Department of Anatomy and Structural Biology, University of Otago, Dunedin, New Zealand.

#### GRANTS

This work was supported by the Centre National de la Recherche Scientifique and Fondation de France to T. Boraud and the Association France Parkinson and Boehringer-Ingelheim Fond to C. Dejean.

## REFERENCES

- Agid Y. Parkinson's disease: pathophysiology. *Lancet* 337: 1321–1323, 1991.
  Albin RL, Young AB, Penney JB. The functional anatomy of basal ganglia disorders. *Trends Neurosci* 12: 366–375, 1989.
- Bartho P, Hirase H, Monconduit L, Zugaro M, Harris KD, Buzsaki G. Characterization of neocortical principal cells and interneurons by network interactions and extracellular features. *J Neurophysiol* 92: 600–608, 2004.
- **Belluscio MA, Kasanetz F, Riquelme LA, Murer MG.** Spreading of slow cortical rhythms to the basal ganglia output nuclei in rats with nigrostriatal lesions. *Eur J Neurosci* 17: 1046–1052, 2003.
- **Belluscio MA, Riquelme LA, Murer MG.** Striatal dysfunction increases basal ganglia output during motor cortex activation in parkinsonian rats. *Eur J Neurosci* 25: 2791–2804, 2007.
- Bergman H, Wichmann T, Karmon B, DeLong MR. The primate subthalamic nucleus. II. Neuronal activity in the MPTP model of parkinsonism. *J Neurophysiol* 72: 507–520, 1994.
- Berke JD, Okatan M, Skurski J, Eichenbaum HB. Oscillatory entrainment of striatal neurons in freely moving rats. *Neuron* 43: 883–896, 2004.
- **Bevan M, Magill P, Terman D, Bolam J, Wilson C.** Move to the rhythm: oscillations in the subthalamic nucleus-external globus pallidus network. *Trends Neurosci* 25: 525–531, 2002.
- Bezard E, Dovero S, Prunier C, Ravenscroft P, Chalon S, Guilloteau D, Bioulac B, Brotchie JM, Gross CE. Relationship between the appearance of symptoms and the level of nigrostriatal degeneration in a progressive MPTP-lesioned macaque model of Parkinson's disease. *J Neurosci* 21: 6853–6861, 2001.
- Boraud T, Brown T, Goldberg JA, Graybiel AM, PJM. Oscillations in the basal banglia: the good, the bad and the unexpected. In: *The Basal Ganglia* (8th ed.), edited by Bolam JP, Ingham CA, Magill PJ. New York: Springer 2005, p. 3–24.
- **Brown P.** Oscillatory nature of human basal ganglia activity: relationship to the pathophysiology of Parkinson's disease. *Mov Disord* 18: 357–363, 2003.
- Day M, Wang Z, Ding J, An X, Ingham CA, Shering AF, Wokosin D, Ilijic E, Sun Z, Sampson AR, Mugnaini E, Deutch AY, Sesack SR, Arbuthnott GW, Surmeier DJ. Selective elimination of glutamatergic synapses on striatopallidal neurons in Parkinson disease models. *Nat Neurosci* 9: 251–259, 2006.
- Degos B, Deniau JM, Thierry AM, Glowinski J, Pezard L, Maurice N. Neuroleptic-induced catalepsy: electrophysiological mechanisms of func-

- tional recovery induced by high-frequency stimulation of the subthalamic nucleus. *J Neurosci* 25: 7687–7696, 2005.
- **Dejean C, Gross CE, Bioulac B, Boraud T.** Synchronous high-voltage spindles in the cortex-basal ganglia network of awake and unrestrained rats. *Eur J Neurosci* 25: 772–784, 2007.
- **DeLong MR.** Primate models of movement disorders of basal ganglia origin. *Trends Neurosci* 13: 281–285, 1990.
- Deransart C, Hellwig B, Heupel-Reuter M, Leger JF, Heck D, Lucking CH. Single-unit analysis of substantia nigra pars reticulata neurons in freely behaving rats with genetic absence epilepsy. *Epilepsia* 44: 1513–1520, 2003
- **Deransart C, Riban V, Le B, Marescaux C, Depaulis A.** Dopamine in the striatum modulates seizures in a genetic model of absence epilepsy in the rat. *Neuroscience* 100: 335–344, 2000.
- **Deransart C, Vercueil L, Marescaux C, Depaulis A.** The role of basal ganglia in the control of generalized absence seizures. *Epilepsy Res* 32: 213–223, 1998.
- **Dunnett SB.** Motor function(s) of the nigrostriatal dopamine system: studies of lesions and behavior. In: *Dopamine*, edited by Dunnett SB, Bentivoglio M, Björklund A, Hökfelt T. Amsterdam: Elsevier, 1983, p. 237–254.
- Fisher NI. Statistical Analysis of Circular Data. New York: Cambridge University Press, 1993.
- Goldberg JA, Boraud T, Maraton S, Haber SN, Vaadia E, Bergman H. Enhanced synchrony among primary motor cortex neurons in the MPTP primate model of Parkinson's disease. *J Neurosci* 22: 4639–4653, 2002.
- **Graybiel AM, Aosaki T, Flaherty AW, Kimura M.** The basal ganglia and adaptive motor control. *Science* 265: 1826–1831, 1994.
- **Hammond C, Bergman H, Brown P.** Pathological synchronization in Parkinson's disease: networks, models and treatments. *Trends Neurosci* 30: 357–364, 2007.
- Hutchison WD, Dostrovsky JO, Walters JR, Courtemanche R, Boraud T, Goldberg J, Brown P. Neuronal oscillations in the basal ganglia and movement disorders: evidence from whole animal and human recordings. J Neurosci 24: 9240–9243, 2004.
- Hyland BI, Reynolds JN, Hay J, Perk CG, Miller R. Firing modes of midbrain dopamine cells in the freely moving rat. *Neuroscience* 114: 475–492, 2002.
- **Kandel A, Buzsáki G.** Cellular-synaptic generation of sleep spindles, spike-and-wave discharges, and evoked thalamocortical responses in the neocortex of the rat. *J Neurosci* 17: 6783–6797, 1997.
- Klausberger T, Magill PJ, Marton LF, Roberts JD, Cobden PM, Buzsaki G, Somogyi P. Brain-state- and cell-type-specific firing of hippocampal interneurons in vivo. *Nature* 421: 844–848, 2003.
- **Kolomiets BP, Deniau JM, Glowinski J, Thierry AM.** Basal ganglia and processing of cortical information: functional interactions between transstriatal and trans-subthalamic circuits in the substantia nigra pars reticulata. *Neuroscience* 117: 931–938, 2003.
- **Kunikowska G, Jenner P.** 6-Hydroxydopamine-lesioning of the nigrostriatal pathway in rats alters basal ganglia mRNA for copper, zinc- and manganese-superoxide dismutase, but not glutathione peroxidase. *Brain Res* 922: 51–64, 2001.
- Leblois A, Meissner W, Bezard E, Bioulac B, Gross CE, Boraud T. Temporal and spatial alterations in GPi neuronal encoding might contribute to slow down movement in Parkinsonian monkeys. Eur J Neurosci 24: 1201–1208, 2006.
- Magill PJ, Bolam JP, Bevan MD. Dopamine regulates the impact of the cerebral cortex on the subthalamic nucleus-globus pallidus network. *Neu-roscience* 106: 313–330, 2001.
- Magill PJ, Sharott A, Bolam JP, Brown P. Brain state-dependency of coherent oscillatory activity in the cerebral cortex and basal ganglia of the rat. J Neurophysiol 92: 2122–2136, 2004.
- Mahon S, Deniau JM, Charpier S. Relationship between EEG potentials and intracellular activity of striatal and cortico-striatal neurons: an in vivo study under different anesthetics. *Cereb Cortex* 11: 360–373, 2001.
- Mallet N, Ballion B, Le Moine C, Gonon F. Cortical inputs and GABA interneurons imbalance projection neurons in the striatum of parkinsonian rats. *J Neurosci* 26: 3875–3884, 2006.
- **Maurice N, Deniau JM, Glowinski J, Thierry AM.** Relationships between the prefrontal cortex and the basal ganglia in the rat: physiology of the cortico-nigral circuits. *J Neurosci* 19: 4674–4681, 1999.

- Meissner W, Leblois A, Hansel D, Bioulac B, Gross CE, Benazzouz A, Boraud T. Subthalamic high frequency stimulation resets subthalamic firing and reduces abnormal oscillations. *Brain* 128: 2372–2382, 2005.
- Murer MG, Riquelme LA, Tseng KY, Pazo JH. Substantia nigra pars reticulata single unit activity in normal and 60HDA-lesioned rats: effects of intrastriatal apomorphine and subthalamic lesions. Synapse 27: 278–293, 1997.
- Murer MG, Tseng KY, Kasanetz F, Belluscio M, Riquelme LA. Brain oscillations, medium spiny neurons, and dopamine. *Cell Mol Neurobiol* 22: 611–632, 2002.
- Nambu A, Tokuno H, Hamada I, Kita H, Imanishi M, Akazawa T, Ikeuchi Y, Hasegawa N. Excitatory cortical inputs to pallidal neurons via the subthalamic nucleus in the monkey. *J Neurophysiol* 84: 289–300, 2000.
- Nini A, Feingold A, Slovin H, Bergman H. Neurons in the globus pallidus do not show correlated activity in the normal monkey, but phase-locked oscillations appear in the MPTP model of parkinsonism. *J Neurophysiol* 74: 1800–1805, 1995.
- **O'Donnell P.** Dopamine gating of forebrain neural ensembles. *Eur J Neurosci* 17: 429–435, 2003.
- **Olsson M, Nikkhah G, Bentlage C, Björklund A.** Forelimb akinesia in the rat parkinson model: differential effects of dopamine agonist and nigral transplants as assessed by a new stepping test. *J Neurosci* 15: 3863–3875, 1995.
- Paxinos G, Watson C. The Rat Brain in Stereotaxic Coordinates New York: Academic Press, 1998.
- Paz JT, Deniau JM, Charpier S. Rhythmic bursting in the cortico-sub-thalamo-pallidal network during spontaneous genetically determined spike and wave discharges. *J Neurosci* 25: 2092–2101, 2005.
- Polack PO, Guillemain I, Hu E, Deransart C, Depaulis A, Charpier S. Deep layer somatosensory cortical neurons initiate spike-and-wave discharges in a genetic model of absence seizures. *J Neurosci* 27: 6590–6599, 2007.
- Robledo P, Féger J. Acute monoaminergic depletion in the rat potentiates the excitatory effect of the subthalamic nucleus in the substantia nigra pars reticulate but not in the pallidal complex. J Neural Transm 86: 115–126, 1991.
- Sharott A, Magill PJ, Harnack D, Kupsch A, Meissner W, Brown P. Dopamine depletion increases the power and coherence of Beta-oscillations in the cerebral cortex and subthalamic nucleus of the awake rat. *Eur J Neurosci* 21: 1413–1422, 2005.
- **Shaw FZ.** Is spontaneous high-voltage rhythmic spike discharge in Long Evans rats an absence-like seizure activity? *J Neurophysiol* 91: 63–77, 2004.
- Slaght SJ, Paz T, Chavez M, Deniau JM, Mahon S, Charpier S. On the activity of the corticostriatal networks during spike-and-wave discharges in a genetic model of absence epilepsy. *J Neurosci* 24: 6816–6825, 2004.
- **Steiner H, Kitai ST.** Unilateral striatal dopamine depletion: time-dependent effects on cortical function and behavioural correlates. *Eur J Neurosci* 14: 1390–1404, 2001.
- **Stern EA, Kincaid AE, Wilson CJ.** Spontaneous subthreshold membrane potential fluctuations and action potential variability of rat corticostriatal and striatal neurons in vivo. *J Neurophysiol* 77: 1697–1715, 1997.
- **Taï CH, Boraud T, Bezard E, Bioulac B, Gross CE, Benazzouz A.** Electrophysiological and metabolic evidence that high frequency stimulation of the subthalamic nucleus bridles neuronal activity in the subthalamic nucleus and the substantia nigra reticulata. *FASEB J* 17: 1820–1830, 2003.
- **Tseng KY, Kargieman L, Gacio S, Riquelme LA, Murer MG.** Consequences of partial and severe dopaminergic lesion on basal ganglia oscillatory activity and akinesia. *Eur J Neurosci* 22: 2579–2586, 2005.
- **Tseng KY, Kasanetz F, Kargieman L, Riquelme LA, Murer MG.** Cortical slow oscillatory activity is reflected in the membrane potential and spike trains of striatal neurons in rats with chronic nigrostriatal lesions. *J Neurosci* 21: 6430–6439, 2001.
- Walters JR, Hu D, Itoga CA, Parr-Brownlie LC, Bergstrom DA. Phase relationships support a role for coordinated activity in the indirect pathway in organizing slow oscillations in basal ganglia output after loss of dopamine. *Neuroscience* 144: 762–776, 2007.
- Wichmann T, Bergman H, Starr PA, Subramanian T, Watts RL, DeLong MR. Comparison of MPTP-induced changes in spontaneous neuronal discharge in the internal pallidal segment and in the substantia nigra pars reticulata in primates. *Exp Brain Res* 125: 397–409, 1999.